

# X

## The $N_c^{-1}$ expansion

The  $N_c^{-1}$  expansion is an attempt to create a perturbative framework for  $QCD$  where none exists otherwise. One extrapolates from the physical value for the number of colors,  $N_c = 3$ , to the limit  $N_c \rightarrow \infty$  while scaling the  $QCD$  coupling constant so that  $g_3^2 N_c$  is kept fixed [’tH 74]. The amplitudes in the theory are then analyzed in powers of  $N_c^{-1}$ . The hope is that the  $N_c \rightarrow \infty$  world bears sufficient resemblance to the real world to yield significant dynamical insights. There is no magical process which makes the  $N_c \rightarrow \infty$  theory analytically trivial; nonlinearities of the nonabelian gauge interactions are present, and the theory is still not solvable. However any consistent approximation scheme for  $QCD$  is welcome, and the large  $N_c$  expansion is especially useful for organizing one’s thoughts in the analysis of hadronic processes.

### X–1 The nature of the large $N_c$ limit

In passing from  $SU(3)$  to  $SU(N_c)$ , the quark and gluon representations, originally **3** and **8**, become  $\mathbf{N}_c$  and  $\mathbf{N}_c^2 - \mathbf{1}$  respectively. The analysis of Feynman graphs at large  $N_c$  is simplified by modifying the notation used to describe gluons. As usual, quarks carry a color label  $j$ , with  $j = 1, 2, \dots, N_c$ . Gluons can be described by two such labels, i.e.

$$A_\mu^a \rightarrow A_{\mu j}^k \quad (A_{\mu j}^j = 0), \quad (1.1)$$

where  $a = 1, \dots, N_c^2 - 1$  and  $j, k = 1, \dots, N_c$ . In doing so, no approximation is being made. The new notation is simply an embodiment of the group product  $\mathbf{N}_c \times \mathbf{N}_c \rightarrow (\mathbf{N}_c^2 - \mathbf{1}) \oplus \mathbf{1}$ . The quark–gluon coupling is then written

$$g_3 \bar{\psi}^j \gamma^\mu \psi_k A_{\mu j}^k, \quad (1.2)$$

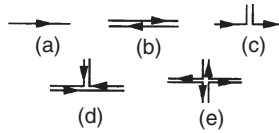


Fig. X-1 Double-line notation: (a) quark and (b) gluon propagators, (c) quark–gluon, (d) three-gluon, and (e) four-gluon vertices.

and the gluon propagator is

$$\int d^4x e^{iq \cdot x} \langle 0 | T (A_{\mu j}^i(x) A_{\nu l}^k(0)) | 0 \rangle = (\delta_l^i \delta_j^k - N_c^{-1} \delta_j^i \delta_l^k) i D_{\mu\nu}(q). \quad (1.3)$$

The term proportional to  $N_c^{-1}$  must be present to ensure that the color singlet combination vanishes,  $A_{\mu j}^j = 0$ . However, as long as we avoid the color-singlet channel, this term will be suppressed in the large  $N_c$  limit and may be dropped when working to leading order.

Using this new notation, the Feynman diagrams for propagators and vertices are displayed in Fig. X-1. A solid line is drawn for each color index, and each gluon is treated as if it were a quark–antiquark pair (as far as color is concerned). In this double-line notation, certain rules which are obeyed by amplitudes to leading order in  $1/N_c$  emerge in an obvious manner. Although general topological arguments exist, we shall review these rules by examining the behavior of specific graphs. The power of Feynman diagrams to build intuition is rather compelling in this case.

We consider first the familiar quark and gluon propagators. The quark propagator, unadorned by higher-order corrections, is  $\mathcal{O}(1)$  in the  $N_c \rightarrow \infty$  limit. Fig. X-2 depicts two radiative corrections. Fig. X-2(a), the one-gluon loop, is  $\mathcal{O}(1)$  in powers of  $N_c$  because the suppression from the squared coupling  $g_3^2$  is compensated for by the single closed loop, which corresponds to a sum over a free color index and thus contributes a factor of  $N_c$ . The graph then is of order  $g_3^2 N_c$ , which is taken to be constant. The graph Fig. X-2(b) with overlapping gluon loops is  $\mathcal{O}(N_c^{-2})$  because, with no free color loops, it is of order  $g_3^4 = (g_3^2 N_c)^2 N_c^{-2} \sim N_c^{-2}$ . The terms *planar* and *nonplanar* are used, respectively, to describe Figs. X-2(a),(b), because the latter cannot be drawn in the plane without at least some internal lines crossing each other.

Four distinct contributions to the gluon propagator are exhibited in Fig. X-3. Figs. X-3(a),(b) depict in double line notation the quark–antiquark and two-gluon



Fig. X-2 Radiative corrections to the quark propagator: (a) planar, (b) nonplanar.

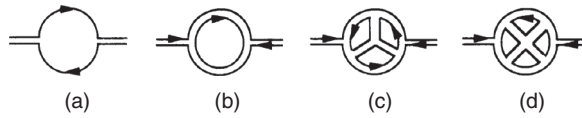


Fig. X-3 Various radiative corrections to the gluon propagator.

loop contributions. It should be obvious from the above discussion that these are respectively  $\mathcal{O}(N_c^{-1})$  and  $\mathcal{O}(1)$ . A new diagram, involving the three-gluon coupling, appears in Fig. X-3(c). With three color loops and six vertices, it is of order  $(g_3^2 N_c)^3 = \mathcal{O}(1)$ . Figure X-3(d) is a nonplanar process with six vertices and one color sum, and is thus  $\mathcal{O}(N_c^{-2})$ .

The discussion of the gluon propagator indicates why we constrain  $g_3^2 N_c$  to be fixed when taking the large  $N_c$  limit. The beta function of QCD is determined to leading order by Figs. X-3(a),(b). If  $g_3^2$  were held fixed, the beta function would become infinite in the large  $N_c$  limit, leading to the immediate onset of asymptotic freedom. The choice  $g_3^2 N_c \sim \text{constant}$  leads to a running coupling constant and is compatible with the behavior for the realistic case of  $N_c = 3$ .

To summarize, there are several rules which can be abstracted from examples such as these: (i) the leading-order contributions are planar diagrams containing the minimum number of quark loops; (ii) each internal quark loop is suppressed by a factor of  $N_c^{-1}$ ; and (iii) nonplanar diagrams are suppressed by factors of  $N_c^{-2}$ . The suppressions in rules (ii), (iii) are combinatorial in origin. Quark loops and nonplanarities each limit the number of color-bearing intermediate states, and consequently cost factors of  $N_c^{-1}$ .

### X-2 Spectroscopy in the large $N_c$ limit

In order for the large  $N_c$  limit to be relevant to the real world, it must be assumed that confinement of color-singlet states continues to hold. In this case, we expect the particle spectrum to continue to be divided into mesons and baryons. Let us treat the mesons first.

One can form color-singlet meson contributions from  $Q\bar{Q}$  pairs. To form a color singlet, one must sum over the quark colors. In order to produce a properly normalized  $Q\bar{Q}$  state one must therefore include a normalization factor of  $N_c^{-1/2}$  into each  $Q\bar{Q}$  meson wavefunction, such that

$$|Q^{(\alpha)}\bar{Q}^{(\beta)}\rangle_{\text{color singlet}} \sim \frac{1}{\sqrt{N_c}} b_i^{(\alpha)\dagger} d_i^{(\beta)\dagger} |0\rangle, \tag{2.1}$$

where  $\alpha, \beta$  are flavor labels,  $i = 1, \dots, N_c$  is the color label, and  $b^\dagger$  ( $d^\dagger$ ) are the quark (antiquark) creation operators. Meson propagators, as represented in

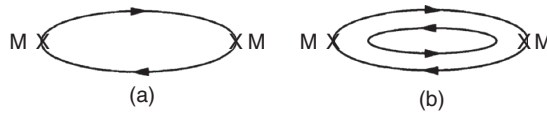


Fig. X-4 Mesons in the double line notation.

Fig. X-4(a), are then  $\mathcal{O}(1)$  in  $N_c$  since the factors of  $(N_c^{-1/2})^2$  from the normalization of the wavefunction are compensated by a factor of  $N_c$  from the quark loop. This leads to the prediction that meson masses are of  $\mathcal{O}(1)$  in the large  $N_c$  limit, i.e., they remain close to their physical values. Multi-quark intermediate states, as in Fig. X-4(b), are suppressed by  $1/N_c$ , indicating a suppression of mixing between  $Q\bar{Q}$  and  $Q^2\bar{Q}^2$  sectors. That is, large  $N_c$  plus confinement implies the existence of  $Q\bar{Q}$  mesons which contain an arbitrary amount of glue in their wavefunction, but which do not mix with  $Q^2\bar{Q}^2$  states.

The quark content of a given hadron remains an issue of some theoretical and phenomenological interest. Several examples are given in Sect. XIII-4 of hadron states which are thought to be ‘nonconventional’. One such is the  $\sigma$  hadron, which is the lightest resonance found in  $\pi\pi$  scattering. Analysis has yielded insight as to the  $N_c$  dependence of the  $\sigma$  mass (cf. Eq. (XIII-4.7)). We reserve further comment on this interesting topic to Chap. XIII.

What about the decay widths of  $Q\bar{Q}$  mesons? The decay amplitude is pictured in Fig. X-5 (other possibilities involve the suppressed quark loops). This diagram contains three meson wavefunctions and one quark loop and hence is of order  $(N_c^{-1/2})^3 N_c = N_c^{-1/2}$  in amplitude or  $N_c^{-1}$  in rate. The large  $N_c$  limit thus involves narrow resonances, i.e.,  $\Gamma/M \rightarrow 0$ , where  $\Gamma$  is the meson decay width and  $M$  is the meson mass. This is reasonably similar to the real world, where most of the observed resonances have  $\Gamma/M \sim 0.1-0.2$  [RPP 12].

Color-singlet gluonic states, called *glueballs*, may also exist. The normalization of a glueball state can be fixed by means of the following argument. Suppose, as will be defined in a gauge-invariant manner in Sect. XIII-4, that a neutral meson can be created from two gluons. Then in normalizing this configuration, one must sum over the  $N_c^2$  gluon color labels. As a consequence, a normalization factor  $N_c^{-1}$  is associated with each glueball state. Glueball propagators also emerge as being  $\mathcal{O}(1)$ . There is no physical distinction between two-gluon states, three-gluon states,

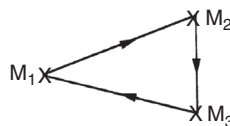


Fig. X-5 Strong interaction decay of a  $Q\bar{Q}$  meson.

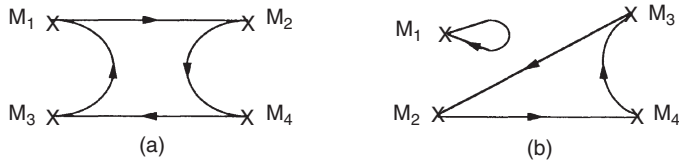


Fig. X-6 Meson–meson scattering.

etc., because all are mixed with each other by the strong interaction. As a result, there need not be any simple association between a specific physical state and gluon number, and thus the concept of a ‘constituent gluon’ need not be inferred. In glueball decays, however, one must distinguish between glueballs decaying to other glueballs, and those decaying to  $Q\bar{Q}$  mesons. Where kinematically allowed, the decay of glueballs to glueballs is  $\mathcal{O}(1)$ , while that to  $Q\bar{Q}$  states is  $\mathcal{O}(1/N_c)$ . The lowest-lying glueball(s) will then be narrow, while those above the threshold for decay into two glueballs will be of standard, nonsuppressed width.

Meson–meson scattering amplitudes are also restricted by large  $N_c$  counting rules. Consider the diagrams of Fig. X-6. That of Fig. X-6(a) is of order  $(N_c^{-1/2})^4 N_c \sim N_c^{-1}$ , whereas Fig. X-6(b) is  $\mathcal{O}(N_c^{-2})$  because of the extra quark loop. The scattering amplitudes thus vanish in the large  $N_c$  limit, and the leading contributions are connected, planar diagrams.

The large  $N_c$  limit also predicts that neutral mesons (i.e.,  $Q^{(\alpha)}\bar{Q}^{(\beta)}$ ) composites with  $\alpha = \beta$ ) do not mix with each other. The possible mixing diagram is given in Fig. X-7, and includes any number of gluons. However, because of the extra quark loop, it is of order  $N_c^{-1}$ , and thus vanishes in the infinite color limit. This means that  $u\bar{u}$  states do not mix with  $d\bar{d}$  or  $s\bar{s}$ , nor do the latter two mix. The large  $N_c$  spectrum thus displays a nonet structure with the  $u\bar{u}$  and  $d\bar{d}$  states degenerate (to the extent that electromagnetism and the mass difference between the  $u$  and  $d$  quarks are neglected) and the  $s\bar{s}$  states somewhat heavier. This pattern is reflected in Nature, except that the  $\bar{u}u$  and  $\bar{d}d$  configurations now appear as states of definite isospin,  $\bar{u}u \pm \bar{d}d$ . For example, let us consider the  $J^{PC} = 1^{--}, 2^{++}$  mesons. For the former,  $\rho(770)$  and  $\omega(783)$  are interpreted as  $u\bar{u}, d\bar{d}$  isospin  $I = 1$  and  $I = 0$  combinations, while  $\phi(1020)$  is the  $s\bar{s}$  member of the nonet. Including the  $K^*(892)$  doublet as the  $\bar{u}s, \bar{d}s$  combinations, a simple additivity in the quark mass would imply

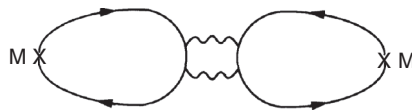


Fig. X-7 Meson–meson mixing.

$$m_{\varphi(1020)} - m_{\rho(770)} = 2(m_{K^*(892)} - m_{\rho(770)}), \quad (2.2)$$

which works well. A similar treatment of the  $2^{++}$  mesons, identifying  $a_2(1320)$  and  $f_2(1270)$  as the corresponding  $u\bar{u}$ ,  $d\bar{d}$  states and  $f'_2(1525)$  as an  $s\bar{s}$  composite, predicts

$$m_{f'_2(1525)} - m_{a_2(1320)} = 2(m_{K_2^*(1430)} - m_{a_2(1320)}), \quad (2.3)$$

which is also approximately satisfied. The fact that  $\rho(770)$ ,  $\omega(783)$ ,  $f_2(1270)$  and  $a_2(1320)$  decay primarily to pions, and  $\varphi(1020)$  and  $f'_2(1525)$  decay primarily to kaons, reinforces this interpretation.

The world of baryons in the large  $N_c$  limit is quite different from that of mesons and glueballs [DaJM 94, Je 98]. In order to form a color singlet, one needs to combine not three quarks but rather  $N_c$  quarks in a totally color-antisymmetric fashion. This forces the baryon mass to grow as  $N_c$ , i.e., to become infinitely heavy in the  $N_c \rightarrow \infty$  limit. In an attempt to model this behavior, it has been suggested that baryons can be associated with the soliton solution, called the *Skyrmion*, of a certain chiral lagrangian [Sk 61, Wi 83b]. We shall discuss this idea in Sect. XI-4 in the context of a model with  $SU(2)_L \times SU(2)_R$  symmetry.

### X-3 Goldstone bosons and the axial anomaly

As stated in the previous section, it must be assumed that color confinement continues to hold in the large  $N_c$  limit. Given this behavior, it can be proven under reasonable conditions that chiral symmetry is spontaneously broken [CoW 80]. In this circumstance, the large  $N_c$  limit turns out to imply a fascinating unity between the  $\eta'(960)$  meson and the octet of Goldstone bosons in massless *QCD* [Wi 79]. The  $N_c = \infty$  analog of  $\eta'(960)$  is *also* a Goldstone boson if quarks are massless.

In order to see this, let us first consider the pseudoscalar decay constants. Because the axial-current matrix elements

$$\langle P_j(\mathbf{q}) | A_k^\mu(0) | 0 \rangle = -i F_j q^\mu \delta_{jk} \quad (3.1)$$

involve one meson normalization factor and one quark loop, they are of order  $(N_c^{-1/2})N_c \sim N_c^{1/2}$ , which then implies  $F_j = \mathcal{O}(N_c^{1/2})$ . Now consider the current divergence in the limit of massless quarks. In general, we have

$$\langle P_j(\mathbf{q}) | \partial_\mu A_k^\mu(0) | 0 \rangle = F_j m_j^2 \delta_{jk}. \quad (3.2)$$

For the octet of currents, the divergence vanishes for zero quark mass, and as usual leads to the identification of  $\pi$ ,  $K$ ,  $\eta_8$  as Goldstone bosons. However, for the singlet

current the anomaly is present. Even in the limit of vanishing quark mass, the current divergence has nonzero matrix elements, in particular,

$$\langle \eta^0(\mathbf{q}) | \partial_\mu A_0^\mu(0) | 0 \rangle = F_{\eta^0} m_{\eta^0}^2 = \left\langle \eta^0(\mathbf{q}) \left| \frac{3g_3^2}{32\pi^2} F_{\mu\nu}^a \tilde{F}^{a\mu\nu} \right| 0 \right\rangle. \tag{3.3}$$

If one repeats the calculation of the anomalous triangle diagram as in Sect. III–3 but now allows  $N_c$  to be arbitrary, one sees that it is proportional to  $\text{Tr}(\lambda^a \lambda^b) = 2\delta^{ab}$  and is therefore independent of  $N_c$ . However, by using large  $N_c$ -counting rules, the matrix element in Eq. (3.3) is seen to be of order  $g_3^2 N_c^{1/2} \sim N_c^{-1/2}$ .<sup>1</sup> This implies that the gluonic contribution to the axial anomaly *vanishes* in the large  $N_c$  limit. When we take into account the behavior of  $F_{\eta'}$ , we conclude that  $m_{\eta'}^2 \sim 1/N_c \rightarrow 0$ . The  $\eta'$  is thus massless in the large  $N_c$  limit, and we end up with a *nonet* of Goldstone bosons.

To illustrate what happens when the number of colors is treated perturbatively, let us consider the  $1/N_c$  corrections to the meson spectrum together with the effects of quark masses. If we first add quark masses, we have, in analogy with the results of Sect. VII–1, the mass matrix

$$m_{ij}^2 = \langle P_i | \hat{m}(\bar{u}u + \bar{d}d) + m_s \bar{s}s | P_j \rangle, \tag{3.4}$$

where we have taken  $m_u = m_d = \hat{m}$ . This leads to a squared-mass matrix

$$\mathbf{m}^2 = B_0 \begin{pmatrix} 2\hat{m} & 0 & 0 & 0 \\ 0 & m_s + \hat{m} & 0 & 0 \\ 0 & 0 & \frac{2}{3}(2m_s + \hat{m}) & \frac{2\sqrt{2}}{3}(\hat{m} - m_s) \\ 0 & 0 & \frac{2\sqrt{2}}{3}(\hat{m} - m_s) & \frac{2}{3}(m_s + 2\hat{m}) \end{pmatrix} \tag{3.5}$$

in the basis  $(\pi, K, \eta_8, \eta_0)$ . If this were diagonalized, one would find an isoscalar state degenerate with the pion. This is a manifestation of the  $U(1)$  problem, which arises when there is no anomaly. However, at the next order in large  $N_c$ , the matrix picks up an extra contribution in the  $SU(3)$ -singlet channel due to the anomaly, yielding

$$\mathbf{m}^2 = B_0 \begin{pmatrix} 2\hat{m} & 0 & 0 & 0 \\ 0 & m_s + \hat{m} & 0 & 0 \\ 0 & 0 & \frac{2}{3}(2m_s + \hat{m}) & \frac{2\sqrt{2}}{3}(\hat{m} - m_s) \\ 0 & 0 & \frac{2\sqrt{2}}{3}(\hat{m} - m_s) & \frac{2}{3}(m_s + 2\hat{m}) + \frac{\epsilon}{N_c B_0} \end{pmatrix}, \tag{3.6}$$

<sup>1</sup> This result depends on the assumption that topologically nontrivial aspects of vacuum structure are smooth in the  $N_c \rightarrow \infty$  limit.

where  $\epsilon = \mathcal{O}(N_c^0)$ . This mass matrix yields an interesting prediction. The quantities  $B_0\hat{m}$  and  $B_0m_s$  are fixed as usual by using the  $\pi$  and  $K$  masses. Also the trace of the full matrix must yield  $m_\pi^2 + m_K^2 + m_\eta^2 + m_{\eta'}^2$ , which fixes  $\epsilon = 2.16 \text{ GeV}^2$ . The remaining diagonalization then predicts  $m_{\eta'} = 0.98 \text{ GeV}$ ,  $m_\eta = 0.50 \text{ GeV}$  with a mixing angle of  $18^\circ$ . This is a remarkably accurate representation of the situation in the real world. Although  $\epsilon/N_c$  is suppressed in a technical sense, note how large it actually is. One is hard pressed to imagine any sense in which the physical  $\eta'$  mass can be taken as a small parameter.

### X-4 The OZI rule

In the 1960s, an empirical property, called the Okubo–Zweig–Iizuka (OZI) rule [Ok 63, Zw 65, Ii 66], was developed for mesonic coupling constants. Its usual statement is that flavor-disconnected processes are suppressed compared to those in which quark lines are connected. In the language which we are using here, flavor disconnected processes are those with an extra quark loop. Unfortunately, the phenomenological and theoretical status of this so-called rule is ambiguous. We briefly describe it here because it is part of the common lore of particle physics.

The empirical motivation for the OZI rule is best formulated in the decays of mesons. Let us accept that  $\varphi(1020)$  and  $f'_2(1525)$  are primarily states with content  $\bar{s}s$  whereas  $\omega(783)$  and  $f_2(1270)$  have content  $(\bar{u}u + \bar{d}d)/\sqrt{2}$ . Mixing between the  $\bar{s}s$  and nonstrange components can take place with a small mixing angle, such that

$$\frac{\text{Amp}(\bar{s}s)}{\text{Amp}([\bar{u}u + \bar{d}d]/\sqrt{2})} \equiv \tan \theta, \tag{4.1}$$

with  $\theta = \theta_V$  for the vector mesons and  $\theta = \theta_T$  for the tensor mesons. In both cases,  $\theta$  is small. Experimentally, the  $\varphi$  and  $f'_2$  decay dominantly into strange particles even though phase space (abbreviated as ‘p.s.’ below) considerations would strongly favor nonstrange modes,

$$\begin{aligned} \frac{\Gamma_{\varphi \rightarrow 3\pi + \rho\pi}}{\Gamma_{\varphi \rightarrow K\bar{K}}} &\simeq 0.18, & \frac{\Gamma_{\varphi \rightarrow 3\pi + \rho\pi}}{\Gamma_{\omega \rightarrow 3\pi}} &\simeq 0.09, \\ \frac{\Gamma_{f'_2 \rightarrow \pi\pi}}{\Gamma_{f'_2 \rightarrow K\bar{K}}} &= 0.012 \pm 0.002 & \frac{\Gamma_{f'_2 \rightarrow \pi\pi}}{\Gamma_{f_2 \rightarrow \pi\pi}} &= 0.004 \pm 0.001 \\ &\simeq 0.003 \times \text{p.s.}, & &\simeq 0.002 \times \text{p.s.} \end{aligned} \tag{4.2}$$

This suggests the hypothesis ‘ $\bar{s}s$  states do not decay into final states not containing strange quarks’. Diagrammatically this leads to a pictorial representation of the



Fig. X-8 *OZI* (a) allowed, (b) forbidden amplitudes.

*OZI* rule, viz., the dominance of Fig. X-8(a) over Fig. X-8(b). Some scattering processes also show such a suppression. For example, we have

$$\frac{\sigma_{\pi^- p \rightarrow \varphi n}}{\sigma_{\pi^- p \rightarrow \omega n}} \simeq 0.03, \tag{4.3}$$

which can be interpreted as an *OZI* suppression. A stronger version of the *OZI* rule would have the  $\varphi/\omega$  and  $f'_2/f_2$  ratios equal to a *universal* factor of  $\tan^2 \theta$  (cf. Eq. (4.1)) once kinematic phase space factors are extracted.

The narrow widths of the  $J/\psi$  and  $\Upsilon$  states are also cited as evidence for the *OZI* rule, since these hadronic decays involve the annihilation of the  $c\bar{c}$  or  $b\bar{b}$  constituents. This can be correct almost as a matter of definition, but it is not very enlightening. Indeed, the small widths of heavy-quark states can be understood within the framework of perturbative *QCD* without invoking any extra dynamical assumptions. However, perturbative *QCD* certainly cannot explain the *OZI* rule in light mesons. It must have a different explanation for these states.

There actually exist several empirical indications counter to the *OZI* rule [Li 84, ELGK 89, RPP 12]. Among the more dramatic examples of *OZI*-forbidden reactions, expressed as ratios, are

$$\begin{aligned} \frac{\Gamma_{J/\psi \rightarrow \varphi \pi^+ \pi^-}}{\Gamma_{J/\psi \rightarrow \varphi K^+ K^-}} &= 1.2 \pm 0.5, & \frac{\sigma_{\gamma p \rightarrow p \varphi \pi^+ \pi^-}}{\sigma_{\gamma p \rightarrow p \omega K^+ K^-}} &= 2.0 \pm 0.7, \\ \frac{\sigma_{\pi^- p \rightarrow f'_2 n}}{\sigma_{\pi^- p \rightarrow f_2 n}} &= 0.23^{+0.14}_{-0.13}, & \frac{\sigma_{\gamma p \rightarrow p \varphi \pi^+ \pi^-}}{\sigma_{\gamma p \rightarrow p \varphi K^+ K^-}} &\geq 5 \text{ (90\% C.L.)}. \end{aligned} \tag{4.4}$$

The universal-mixing model is incorrect more often than not, with counterexamples being

$$\begin{aligned} \frac{\Gamma_{J/\psi \rightarrow \varphi \pi^+ \pi^-}}{\Gamma_{J/\psi \rightarrow \omega \pi^+ \pi^-}} &= 0.11 \pm 0.02, & \frac{\sigma_{\gamma p \rightarrow p \varphi \pi^+ \pi^-}}{\sigma_{\gamma p \rightarrow p \omega \pi^+ \pi^-}} &= 0.10 \pm 0.02, \\ \frac{\sigma_{\bar{p} p \rightarrow f'_2 \pi^+ \pi^-}}{\sigma_{\bar{p} p \rightarrow f_2 \pi^+ \pi^-}} &= 0.029^{+0.011}_{-0.007}, \end{aligned} \tag{4.5}$$

instead of the values 0.03, 0.03, and 0.006 expected from the previous ratios. The empirical  $\eta$ - $\eta'$  mixing angle  $\theta_{\eta-\eta'} \simeq -20^\circ$  also violates the *OZI* rule, which would require a mixing angle of  $-35^\circ$ .

There is also an intrinsic logical flaw with the simplest formulation of the *OZI* rule. This is because *OZI*-forbidden processes can take place as the product of two *OZI*-allowed processes. For example, each of the following transitions is *OZI*-allowed:

$$\begin{aligned} f'_2 &\rightarrow K\bar{K}, & K\bar{K} &\rightarrow \pi\pi, \\ f'_2 &\rightarrow \eta\eta, & \eta\eta &\rightarrow \pi\pi. \end{aligned} \quad (4.6)$$

Hence the *OZI*-forbidden reaction  $f'_2 \rightarrow \pi\pi$  can take place by the chains

$$f'_2 \rightarrow K\bar{K} \rightarrow \pi\pi, \quad f'_2 \rightarrow \eta\eta \rightarrow \pi\pi. \quad (4.7)$$

These two-step processes are in fact required by unitarity to the extent that the individual scattering amplitudes are nonzero.

The large  $N_c$  limit provides the only known dynamical explanation of the *OZI* rule at low energies. Although the gluonic coupling constant is not small at these scales and suppressed diagrams have ample energy to proceed, they are predicted to be of order  $1/N_c^2$  in rate because of the extra quark loop. Yet large  $N_c$  arguments need not suggest a universal suppression factor of  $\tan^2\theta$ , because there is no need for the  $1/N_c$  corrections to be universal. Note that the large  $N_c$  framework also forbids the mixing of  $\eta$  and  $\eta'$  and, more generally, the scattering of mesons.

Thus, the *OZI* rule in light-meson systems remains somewhat heuristic. It has a partial justification in large  $N_c$  counting rules, but it also has known violations. It is not possible to predict with certainty whether it will work in any given new application.

### X-5 Chiral lagrangians

The large  $N_c$  limit places restrictions on the structure of chiral lagrangians [GaL 85a]. To describe these, we must first allow for an enlarged number  $N_f > 3$  of quark flavors. The three-flavor  $\mathcal{O}(E^4)$  lagrangian is expanded as

$$\mathcal{L}_4 = \sum_{i=1}^{10} L_i O_i, \quad (5.1)$$

where the  $\{O_i\}$  can be read off from Eq. (VII-2.7). Recall that in constructing  $\mathcal{L}_4$ , we removed the  $\mathcal{O}(E^4)$  operator

$$O_0 \equiv \text{Tr} (D_\mu U D_\nu U^\dagger D^\mu U D^\nu U^\dagger), \quad (5.2)$$

because for  $N_f = 3$  it is expressible (cf. Eq. (VII-2.3)) as a linear combination of  $O_{1,2,3}$ . However, if the number of flavors exceeds three, one must append  $O_0$  to the lagrangian of Eq. (5.1),

$$\mathcal{L}_4 = \sum_{i=1}^{10} L_i O_i \xrightarrow{N_f > 3} \sum_{i=0}^3 B_i O_i + \sum_{i=4}^{10} L_i O_i. \tag{5.3}$$

In view of the linear dependence of  $O_0$  on  $O_{1,2,3}$ , note that we have needed to modify the coefficients  $L_{1,2,3} \rightarrow B_{1,2,3}$ . Upon returning to three flavors, we regain the original coefficients,

$$L_1 = \frac{B_0}{2} + B_1, \quad L_2 = B_0 + B_2, \quad L_3 = -2B_0 + B_3. \tag{5.4}$$

We can now study the large  $N_c$  behavior of the extended  $\mathcal{O}(E^4)$  chiral lagrangian. The distinguishing feature is the number of traces in a given  $\mathcal{O}(E^4)$  operator. Each such trace is taken over *flavor* indices and amounts to a sum over the quark flavors, which in turn can arise only in a *quark loop*. In particular, those operators with two flavor traces ( $O_{1,2,4,6,7}$ ) will require at least two quark loops, while those with one flavor trace need only one quark loop. However, our study of the large  $N_c$  limit has taught us that every quark loop leads to a  $1/N_c$  suppression. Thus, the  $\mathcal{O}(E^4)$  chiral contributions having two traces will be suppressed relative to those with one trace by a power of  $1/N_c$ , and provided  $B_3 \neq 0$  we can write<sup>2</sup>

$$\frac{B_1}{B_3} = \frac{B_2}{B_3} = \frac{L_4}{L_3} = \frac{L_6}{B_3} \xrightarrow{N_c \rightarrow \infty} 0. \tag{5.5a}$$

Alternatively, this  $N_c$ -counting rule implies (provided  $B_0/B_3 \neq 1/2$ ) for the  $\{B_i\}$  coefficients of flavor  $SU(3)$ ,

$$\frac{2L_1 - L_2}{L_3} = \frac{L_4}{L_3} = \frac{L_6}{L_3} = \mathcal{O}(N_c^{-1}). \tag{5.5b}$$

The overall power of  $N_c$  for the remaining terms can be found by noting that the  $\pi\pi$  scattering amplitude should be of order  $N_c^{-1}$ , implying  $L_{1,2,3} = \mathcal{O}(N_c)$ .

The only exception to the above counting behavior is the operator with coefficient  $L_7$ . This exception occurs because the operator can be generated by an  $\eta'$  pole, and the  $\eta'$  mass-squared is  $\mathcal{O}(1/N_c)$ . In particular, the coefficient of this term is absolutely predicted in the large  $N_c$  limit. This follows if we include the large  $N_c$  result for mixing between  $\eta$  and  $\eta'$  shown in Eq. (3.6) as a chiral lagrangian

$$\mathcal{L}_{\eta\eta'} = \frac{F_\pi}{2\sqrt{6}} \eta_0 \text{Tr} (\chi^\dagger U - U^\dagger \chi), \tag{5.6}$$

which when expanded to order  $\eta_0\eta_8$  will yield the off-diagonal term in the mass mixing matrix of Eq. (3.6). Integrating out the  $\eta_0 \sim \eta'$  leads to the effective lagrangian

<sup>2</sup> The operator  $O_7$  presents a special case and is discussed below.

$$\mathcal{L}_{\text{eff}} = -\frac{1}{48} \frac{F_\pi^2}{m_{\eta'}^2} \left[ \text{Tr} (\chi^\dagger U - U^\dagger \chi) \right]^2. \tag{5.7}$$

It is the factor of  $m_{\eta'}^{-2}$  which overcomes the counting rules. Although the double trace suggests that this operator is suppressed in the large  $N_c$  limit, we have  $m_{\eta'}^{-2} \propto N_c$ . Thus, at least formally, an extra enhancement would be predicted.

The large  $N_c$  limit then predicts the following ordering of the chiral coefficients in  $\mathcal{L}_4$ :

$$\begin{aligned} L_7 &= \mathcal{O}(N_c^2), \\ L_1, L_2, L_3, L_5, L_8, L_9, L_{10} &= \mathcal{O}(N_c), \\ 2L_1 - L_2, L_4, L_6 &= \mathcal{O}(1). \end{aligned} \tag{5.8}$$

An existing empirical test involves the occurrence of  $2L_1 - L_2$  in  $K \rightarrow \pi\pi e\bar{\nu}_e$  decays [Bi 90, RiGDH 91], and the prediction works quite well. The large  $N_c$  enhancement of  $L_7$  is probably just a curiosity in that the physical value of the  $\eta'$  mass is not small compared to other masses in the theory, and hence the technical advantage of  $m_{\eta'}^2 \propto N_c^{-1}$  is probably not useful phenomenologically.

### Problems

(1) **The large  $N_c$  weak hamiltonian**

Retrace the calculation of the *QCD* renormalization of the weak nonleptonic hamiltonian described in Sect. VIII-3, but now in the limit  $N_c \rightarrow \infty$  with  $g_3^2 N_c$  fixed. Show that the penguin operators do not enter and that all short-distance effects are of order  $N_c^{-1}$ , with the operator-product coefficients  $c_1 = 1$ ,  $c_2 = 1/5$ ,  $c_3 = 2/15$ ,  $c_4 = 2/3$ ,  $c_5 = c_6 = 0$ .

(2) **The strong *CP* problem in the large  $N_c$  limit**

In the large  $N_c$  limit, the  $\eta_0$  can be united with the Goldstone octet in the effective lagrangian. Generalizing the chiral matrix to nine fields we write  $\mathcal{L} = \mathcal{L}_0 + \mathcal{L}_{N_c^{-1}}$ , where

$$\begin{aligned} \mathcal{L}_0 &= \frac{F^2}{4} \text{Tr} \left( \partial_\mu \tilde{U} \partial^\mu \tilde{U}^\dagger \right) + \frac{F^2}{4} B_0 \text{Tr} \left( \mathbf{m}(\tilde{U} + \tilde{U}^\dagger) \right), \\ \mathcal{L}_{N_c^{-1}} &= \frac{\epsilon}{N_c} \frac{F^2}{24} \left[ \text{Tr} (\ln \tilde{U} - \ln \tilde{U}^\dagger) \right]^2, \\ \tilde{U} &= \exp(i\boldsymbol{\lambda} \cdot \boldsymbol{\varphi}/F) \exp\left( i\sqrt{\frac{2}{3}} \frac{\varphi^0}{F} \right). \end{aligned}$$

- (a) Confirm that this reproduces the mixing matrix of Eq. (3.6).  
 (b) Another way to obtain this result is to employ an auxiliary pseudoscalar field  $q(x)$  (with no kinetic energy term) to rewrite  $\mathcal{L}_{N_c^{-1}}$  as

$$\mathcal{L}_{N_c^{-1}} = \frac{N_c}{4\epsilon} q^2(x) + i \frac{F}{2\sqrt{6}} q(x) \text{Tr} (\ln \tilde{U} - \ln \tilde{U}^\dagger).$$

Identify the  $SU(3)$ -singlet axial current and calculate its divergence to show that  $q(x)$  plays the same role as  $F\tilde{F}$ , i.e.,  $q(x) \sim \alpha F\tilde{F}/8\pi$ . Integrate out  $q(x)$  to show that this is equivalent to the form of part (a).

- (c) Several authors [RoST 80, DiV 80] suggest adding the  $\theta$  term through

$$\mathcal{L} = \mathcal{L}_0 + \mathcal{L}_{N_c^{-1}} - \theta q(x).$$

From this starting point, integrate out  $q(x)$  and show that a chiral rotation can transfer  $\theta$  to  $\arg(\det \mathbf{m})$ . However, in the sense described in Sect. IX-4, this theory is unstable about  $\tilde{U} = 1$ . The stable vacuum corresponds to  $\tilde{U}_{jk} = \delta_{jk} \exp(i\beta_j)$ . For small  $\theta$ , solve for  $\beta_j$  in terms of  $\theta$ .

- (d) Using  $\tilde{U} = e^{i\beta/2} U e^{i\beta/2}$ , define the fields about the correct vacuum to find the  $CP$ -violating terms of the form

$$\mathcal{L}_{CP} = i\theta [a \text{Tr} (U - U^\dagger) + b \text{Tr} (\ln U - \ln U^\dagger)],$$

identifying  $a$  and  $b$  and showing they vanish if any quark mass vanishes. Calculate the  $CP$ -violating amplitude for  $\eta \rightarrow \pi^+ \pi^-$ .